

## Photophysics

International Edition: DOI: 10.1002/anie.201804852  
German Edition: DOI: 10.1002/ange.201804852

## Fluorescence Blinking Beyond Nanoconfinement: Spatially Synchronous Intermittency of Entire Perovskite Microcrystals

Nithin Pathoor<sup>+</sup>, Ansuman Halder<sup>+</sup>, Amitrajit Mukherjee, Jaladhar Mahato, Shaibal K. Sarkar,\* and Arindam Chowdhury\*

In memory of Professor Mihir Chowdhury

**Abstract:** Abrupt fluorescence intermittency or blinking is long recognized to be characteristic of single nano-emitters. Extended quantum-confined nanostructures also undergo spatially heterogeneous blinking; however, there is no such precedent in dimensionally unconfined (bulk) materials. Herein, we report multi-level blinking of entire individual organo-lead bromide perovskite microcrystals (volume = 0.1–3  $\mu\text{m}^3$ ) under ambient conditions. Extremely high spatiotemporal correlation (>0.9) in intracrystal emission intensity fluctuations signifies effective communication amongst photo-generated carriers at distal locations (up to ca. 4  $\mu\text{m}$ ) within each crystal. Fused polycrystalline grains also exhibit this intriguing phenomenon, which is rationalized by correlated and efficient migration of carriers to a few transient non-radiative traps, the nature and population of which determine blinking propensity. Observation of spatiotemporally correlated emission intermittency in bulk semiconductor crystals opens the possibility of designing novel devices involving long-range (mesoscopic) electronic communication.

**F**luorescence intermittency or blinking, which refers to temporally random discrete jumps in intensity between bright and dark levels, has been considered as one of the main pieces of evidence for the detection of single nano-sized quantum emitters.<sup>[1–8]</sup> Apart from single molecules, blinking is commonly observed in various individual quantum-confined systems such as semiconductor nanocrystals (NCs), in which excitons/charge carriers are spatially restricted in more than one dimension.<sup>[4–13]</sup> In NCs, photoluminescence (PL) blinking is attributed to intermittent Auger ionization–recombination processes leading to charging–discharging of NCs or long-lived carrier trapping in surface (defect) states.<sup>[4,5,14,15]</sup> However, PL intermittency is seldom observed beyond the

nanoscale (approaching bulk), as temporally uncorrelated intensity fluctuations from various emitters average out over the ensemble and contribution of surface states in radiative recombination becomes less significant compared to that of free carriers in the bulk.<sup>[7]</sup>

Even for 1D- or 2D-confined extended nanostructures, blinking beyond the diffraction limit (ca. 250 nm) is uncommon, and such PL intermittency is spatially heterogeneous, that is, spatiotemporally uncorrelated.<sup>[9,16]</sup> There is a rare example of spatially concerted PL intensity fluctuations in an extended quantum-confined system;<sup>[10]</sup> a small proportion (1–2%) of entire single CdSe quantum wires were found to exhibit correlated multilevel blinking, attributed to delocalized 1D excitons, which allow efficient long-range carrier migration. More recently, individual stacked-monolayers of transition metal dichalcogenides (MoSe<sub>2</sub>/WS<sub>2</sub>) were reported to undergo temporally anti-correlated blinking arising from mobile 2D excitons, which experience sporadic interlayer charge transport.<sup>[17]</sup>

Owing to their exceptional carrier diffusion lengths and diffusivities,<sup>[18,19]</sup> organo-metal (hybrid) perovskites have gained considerable attention as suitable materials for photovoltaics. Hybrid halide perovskite (HHP) nanorods (250 nm in length) have been shown to undergo spatially extended multilevel blinking induced by metastable defects, which efficiently trap photogenerated carriers in close vicinity.<sup>[11,12]</sup> Recently, single-crystal nanorods of HHPs were found to exhibit spatially extended heterogeneous blinking, attributed to mobile charged traps, which transiently quench the emission of the surroundings even beyond the diffraction limit.<sup>[20]</sup> A similar mechanism is likely to be responsible for temporally uncorrelated PL blinking in nanodomains of doped HHP polycrystalline grains.<sup>[21]</sup>

In a quest to explore whether larger HHP crystals can exhibit spatially extended PL intermittency, we investigated methylammonium (MA) lead halide microcrystals (MCs), in which efficient long-range carrier diffusion has been reported.<sup>[18,19]</sup> Herein, we present an extraordinary phenomenon in which individual micron-sized MA lead bromide crystals undergo spatiotemporally correlated PL blinking as single entities. For bulk materials without any dimensional confinement, the observation of spatially synchronous blinking is unprecedented and suggests long-range communication between photogenerated carriers spatially separated far beyond the diffraction limit.

[\*] N. Pathoor,<sup>[†]</sup> A. Mukherjee, J. Mahato, Dr. A. Chowdhury  
Department of Chemistry, Indian Institute of Technology Bombay  
Powai, Mumbai 400076 (India)  
E-mail: arindam@chem.iitb.ac.in

A. Halder,<sup>[†]</sup> Dr. S. K. Sarkar  
Department of Energy Science and Engineering  
Indian Institute of Technology Bombay  
Powai, Mumbai 400076 (India)  
E-mail: shaibal.sarkar@iitb.ac.in

[†] These authors contributed equally to this work.

Supporting information and the ORCID identification number(s) for the author(s) of this article can be found under:  
<https://doi.org/10.1002/anie.201804852>.

$\text{CH}_3\text{NH}_3\text{PbBr}_3$  (MAPbBr<sub>3</sub>) MCs were grown on glass coverslips using a solution processed method, in which the density of the crystals could be controlled by the precursor concentration and spin casting rate. The details of the synthetic and experimental procedures are provided in the Supporting Information. X-Ray diffraction (XRD) and transmission electron microscopy (TEM) data (Figure S1, Supporting Information) corroborate a perovskite structure with polycrystalline grains. Scanning electron microscopy (SEM) image of a typical sample area (Figure 1 a) shows formation of

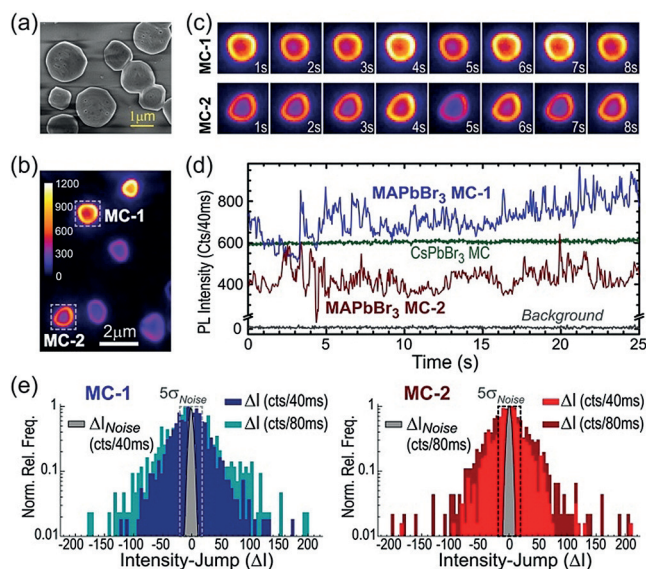


**Figure 1.** PL intermittency of entire isolated MCs. Typical a) SEM and b) PL image of MAPbBr<sub>3</sub> MCs on a glass coverslip. c) Sequential (1 s) PL images of two individual crystals, MC-1 and MC-2 (see Movie M1), d) Integrated PL intensity trajectories of entire MC-1 and MC-2 along with emission intensity fluctuations for an entire single CsPbBr<sub>3</sub> MC and that for the background noise. e) Distribution of emission intensity jumps (per 40 and 80 ms) for MC-1 and MC-2 along with that for the background (see Figure S5, Supporting Information).

quasi-circular disks; however, a few grains are sometimes fused together to form elongated MCs. Atomic force microscopy (AFM) measurements (Figure S2, Supporting Information) reveal that the grains resemble a mesa hundreds of nanometers in height, indicating a dimensionally unconfined bulk material. The solid-state optical spectra (Figure S3, Supporting Information) show an excitonic absorption feature at 520 nm (2.38 eV) and an intense emission peak at 544 nm (2.28 eV), while the average fluorescence lifetime ( $\langle\tau\rangle$ ) is 51 ns (Figure S4, Supporting Information). To investigate the spatiotemporal PL behaviour of MCs, we performed epifluorescence video microscopy (at 25 Hz) under ambient conditions (295 K), for which samples were excited using a 405 nm laser, and the collected emission was imaged using a CCD camera (details provided in Supporting Information).

Fluorescence imaging of MAPbBr<sub>3</sub> MCs (Figure 1b) reveals spatially non-uniform emission from individual grains, with higher intensity at the edges compared to that

at the interiors, similar to recent reports on other perovskites.<sup>[21–23]</sup> Such contrasting behaviour is likely due to differences in electronic structure and radiative recombination dynamics at the boundaries and interior regions of MCs. More interestingly, we find that PL intensity of each MC fluctuates dramatically with time (see Movie M1, Supporting Information), exemplified in Figure 1c using sequential images (over 8 s at 1 s intervals) for two MCs (MC-1 and MC-2). The PL intensity trajectories for entire MAPbBr<sub>3</sub> MCs (Figure 1d) reveal sudden jumps between various dim and bright levels on top of a slow (<1 Hz) time-varying base intensity. The recurrence of high frequency (>10 Hz) prominent PL fluctuations is validated using intensity jump distributions for each MC (Figure 1e), which have significantly larger width compared to that for the background noise. We designate abrupt (40–80 ms) intensity jumps with amplitudes more than five times the standard deviation of the background fluctuations (ca. 4 cts) as blinking (Figure S5, Supporting Information). In stark contrast to MAPbBr<sub>3</sub>, all-inorganic perovskite (CsPbBr<sub>3</sub>) MCs of comparable dimensions do not blink at all (Figure 1d and Figure S6, Supporting Information). It is emphasized that no two segregated MAPbBr<sub>3</sub> MCs in the same movie undergo correlated PL intermittency (Figure 1d and Figure S7, Supporting Information), ruling out external factors such as laser intensity variations as a cause. Neither does blinking arise from temporally random spectral shifts (Figure S8, Supporting Information), nor is it a consequence of pronounced intensity fluctuations only within certain nanodomains, suggestive of spatial homogeneity in blinking dynamics across each crystal.

A comparison of spatially resolved PL trajectories within two larger MCs is shown in Figure 2a. These reveal that nanodomains within each MC exhibit nearly indistinguishable dynamical trends, although blinking amplitudes vary considerably over different spatial locations (Figure S9, Supporting Information). Importantly, temporal overlay of peaks and troughs for the spatially resolved trajectories as well as the respective entire MC, provides compelling evidence that individual crystals undergo correlated blinking as a whole. To quantify spatially synchronous PL fluctuations of each MC, we evaluated the Pearson correlation coefficient (PCC),  $r$ , (see methods, Supporting Information) between intensity trajectories at every location ( $i^{\text{th}}$  pixel) within an MC and that for the entire entity. Using  $r$  values for each pixel ( $r_i$ ), we generated a spatial map of correlation coefficients for individual MCs (Figure 2b). These correlation images show extremely high  $r_i$  values (typically >0.85) over entire MCs (Figure S9, Supporting Information), and sharply fall off to circa 0.2 beyond boundaries. We have analyzed correlation images of 125 single MAPbBr<sub>3</sub> MCs of lateral dimensions between 0.8–9  $\mu\text{m}^2$  (Figure 2c) and found that an overwhelming majority (>95%) have a spatially averaged  $r$  ( $\langle r \rangle$ ) over 0.9 with nominal standard deviations. From the statistical distribution constructed using 125 isolated MCs (Figure S10, Supporting Information), the ensemble average of  $\langle r \rangle$  was found to be  $0.95 \pm 0.04$ , which further demonstrates the incredibly high intracrystal spatiotemporal correlation in PL fluctuations for nearly all MCs up to lateral dimensions of circa 10  $\mu\text{m}^2$ .

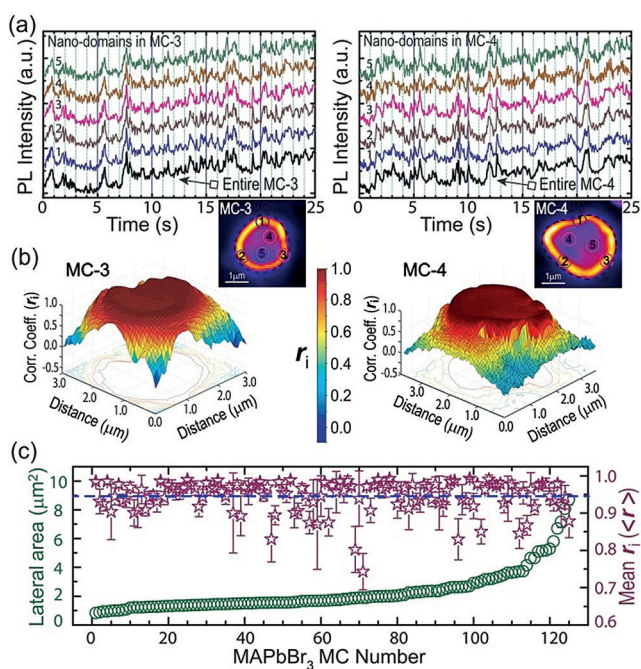


**Figure 2.** Spatially correlated blinking in individual MCs. a) Normalized PL intensity fluctuations from five nanodomains of two MAPbBr<sub>3</sub> MCs (-3 and -4, insets) and the entire MC traces (see Movies M2 and M3). b) Spatial maps of correlation coefficients ( $r_i$ ) for MC-3 and MC-4. c) Spatially averaged intra-crystal  $r_i$  ( $r_i$ ) (stars) and corresponding size (circles) of 125 isolated MCs. Vertical bars depict standard deviation of  $r$  for each MC. Horizontal line represents mean value of the distribution (see Figure S10, Supporting Information).

Spatially synchronous PL blinking of entire micron-sized (bulk) crystals is an unambiguous indicator of extremely long-range ( $> \mu\text{m}$ ) communication amongst carriers photogenerated at diverse spatial locations, which is astounding. This implies that despite MAPbBr<sub>3</sub> being a semiconductor, a large number of carriers are extensively delocalized within each crystal, which in effect determines their collective migration over large distances. Our inference is consistent with high charge carrier diffusivities (ca.  $10^8 \mu\text{m}^2 \text{s}^{-1}$ ) and diffusion lengths (a few micrometers) reported for HHPs.<sup>[18,24]</sup> Furthermore, rarely do we find spatially correlated blinking beyond  $5 \mu\text{m}$  in larger crystals, indicative of a strong connection between entire-MC intermittency and carrier diffusion propensity.

In this context, it is relevant to note that grain boundaries can often hinder carrier diffusion owing to potential barriers created by structural defects.<sup>[25]</sup> To probe the effect of grain boundaries, we inspected relatively large, elongated MAPbBr<sub>3</sub> MCs with conjoined grains (see Figure 1a). The PL image of such an MC is shown in Figure 3a, in which four fused grains (I–IV) can be readily identified by their prominent edges. Spatially integrated PL trajectories (Figure 3b, top) reveal that all these grains collectively blink in unison (Movie M4, Supporting Information). However, segregated grains (such as V) in close proximity does not (Figure 3b, bottom). Concerted blinking of fused grains (I–IV) is validated by very high inter-grain PCC (0.85–0.93), in contrast to nominal value (0.22) for disjointed grains (Fig-

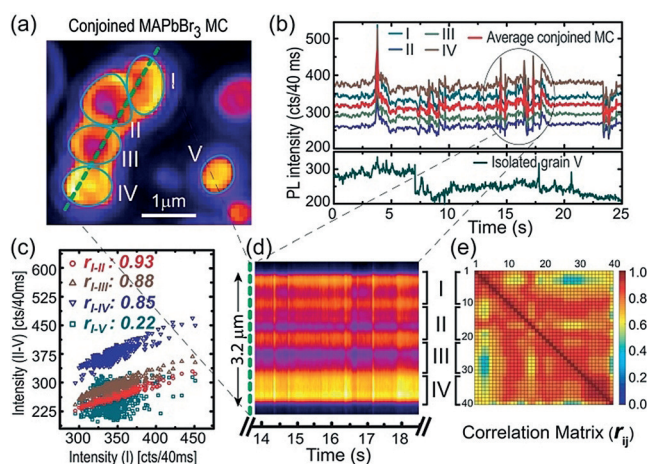


**Figure 3.** Concerted blinking of conjoined MC grains. a) An elongated MAPbBr<sub>3</sub> MC with fused grains (I–IV) and a disjointed grain (V) nearby. b) Synchronous blinking dynamics of I–IV and entire fused MC (top) in contrast to V (bottom) (see Movie M4). c) Integrated intensities of II–V against I for each frame and corresponding correlation coefficients. d) Spatially resolved intensity trajectory and e) correlation coefficient matrix for each pair of pixels, along the  $3.2 \mu\text{m}$ -long strip traversing the fused MC grains.

ure 3c). Moreover, spatial correlation in blinking progressively decreases, albeit slightly, with inter-grain distance, indicating marginal decrease in communication amongst carriers in grains located farther from one another.

To evaluate the spatial variation in the extent of correlated blinking, we plotted the temporal evolution of PL intensity along a strip spanning the fused MC (Figure 3d). We find that abrupt intensity fluctuations always occur in-synch over the entire strip, although slow temporal modulations in base intensity are not necessarily uniform. Using the spatially resolved intensity trajectories, we generated a PCC matrix ( $r_{ij}$ ) for each pair of pixels (i and j) (see methods, Supporting Information), in which off-diagonal elements represent the extent of inter-pixel blinking correlation (Figure 3e). High  $r_{ij}$  values ( $> 0.8$ ) corroborate that the majority of nanodomains in the strip blink in concert. Intriguingly, the blinking correlation does not diminish uniformly with distance between pixels; there are few localized zones for which correlation is modest ( $r_{ij} \approx 0.6 \pm 0.1$ ). This is primarily due to non-uniform slow ( $> \text{second}$ ) intensity modulations at certain local regions rather than the occurrence of spatiotemporally incoherent blinking events. We find that a majority (ca. 60%) of fused MC grains undergo concerted blinking over extended regions (up to ca.  $10 \mu\text{m}^2$ ), while the remaining ones exhibit sporadic spatially uncorrelated blinking (Figure S11, Supporting Information), the precise reasons for which remain elusive.

While there are variations in blinking dynamics amongst individual MCs in the ensemble, the frequency of PL intermittency is nominally affected by the excitation power ( $0.1\text{--}10 \text{ W cm}^{-2}$ ) or photon energy ( $405\text{--}532 \text{ nm}$ ). It is therefore unlikely that blinking in bulk crystals involves Auger ionization or surface trapping of charges. We propose a phenomenological model for multi-level blinking of entire

MAPbBr<sub>3</sub> MCs. First, prominent PL intensity fluctuations involve creation and removal of defects, which can temporarily quench the emission in their vicinity.<sup>[2,11]</sup> The absence of spectral diffusion upon blinking (Figure S6, Supporting Information) suggests that metastable defects are nonradiative (NR) energetic funnels (traps). Second, spatially correlated intensity fluctuations in MAPbBr<sub>3</sub> must be intricately related to effective communication amongst a majority of carriers throughout entire MCs. Extensive delocalization of charge-carrier wavefunctions<sup>[10]</sup> and/or strong correlation amongst photogenerated carriers is likely to play a significant role in such communication processes. In effect, carriers generated at any location can recognize the transiently formed NR traps within an MC, and high carrier diffusivities (ca.  $10^8 \mu\text{m}^2\text{s}^{-1}$ ) in MAPbBr<sub>3</sub> permit fast (ca. hundreds of nanoseconds) carrier migration to distal (on the order of micrometers) NR traps. As a consequence, the PL emission for entire MC grains is abruptly quenched. Upon annihilation or passivation of metastable traps, carriers generated at various locations are unable to access certain NR channels, and thus, PL intensity is (momentarily) augmented throughout individual MCs. Since prominent PL intensity fluctuations of entire crystals occur at circa 100 ms, the process of NR trap formation and annihilation ought to take place at comparable timescales, much slower than that for correlated migration of carriers.

To verify whether entire MC blinking involves mesoscale carrier migration, we probed the PL emission from conjoined MCs through regioselective excitation. We find significant emission emanates from entire unilluminated (adjacent) fused-grains (Figure S12, Supporting Information), which provides concrete evidence that carriers can migrate over a few micrometers before recombining radiatively. It is important to note that owing to shorter average radiative-recombination lifetimes ( $\langle\tau\rangle \approx 51$  ns) (Figure S4, Supporting Information) compared to the timescales of correlated carrier migration, entire MC PL blinking always occurs on top of a dominant base intensity level. Moreover, multi-level intermittency with a wide distribution of fluctuation amplitudes is likely to arise from a few metastable traps, each of which can partially quench the emission of an entire single MC to a different extent.<sup>[11]</sup> We surmise that spatiotemporal variation in NR trap population leads to diverse blinking dynamics for different MCs in the ensemble, as well as for each MC at different time windows. We have preliminary evidence that the metastable NR traps, at least in part, originate from adsorption/desorption of environmental constituents such as moisture; measurements performed under controlled environments reveal that entire-MC blinking is initiated only above a threshold relative humidity (ca. 30%) and is augmented in the presence of oxygen.<sup>[26]</sup> While further studies are necessary to completely elucidate entire-MC blinking—identifying the exact nature of metastable quenchers as well as the specific role of organic (MA) cations, our results hopefully, will stimulate others to propose alternate plausible mechanisms.

To conclude, we report a unique phenomenon of spatially correlated fluorescence blinking of entire individual MCs of MAPbBr<sub>3</sub>. Our results demonstrate that polycrystalline bulk

materials can also undergo multi-level blinking, which dispels the long-standing notion that nanoscale carrier confinement is essential to exhibit fluorescence intermittency. Spatial synchronicity of intracrystal blinking has profound implications; this is a clear indicator of extremely long-range (a few microns) communication amongst a majority of photogenerated carriers, which can potentially be harnessed for novel device or sensing applications. We propose that entire-crystal blinking originates from mesoscopic correlated migration of charge carriers to a few metastable nonradiative traps; however, a comprehensive understanding of the mechanism is necessary. Visualization of intra-microcrystal concerted intermittency opens an avenue to estimate the lower bounds of carrier diffusion parameters in bulk perovskites as well as other dimensionally unconfined semiconductor microstructures.

### Acknowledgements

Financial support provided by Solar Energy Research Institutes of India and US (SERIUS) and Ministry of New and Renewable Energy (MNRE), Govt. of India. A.C. thanks the National Center for Photovoltaic Research and Education (NCPRE), aided by MNRE for partial financial support. Authors acknowledge IRCC and CRNTS, IIT Bombay for usage of central facility equipment. N.P. and A.M. acknowledge fellowships from CSIR (India). A.C. thanks Subhabrata Dhar, Siuli Mukhopadhyay, Amitabha Tripathi, and the Kaleidoscope-2017 meeting for valuable discussions.

### Conflict of interest

The authors declare no conflict of interest.

**Keywords:** correlated carrier migration · concerted blinking · hybrid perovskites · long-range communication · transient traps

**How to cite:** *Angew. Chem. Int. Ed.* **2018**, *57*, 11603–11607  
*Angew. Chem.* **2018**, *130*, 11777–11781

- [1] X. S. Xie, R. C. Dunn, *Science* **1994**, *265*, 361–364.
- [2] D. A. Vanden Bout, W. Yip, D. Hu, D. Fu, T. M. Swager, P. F. Barbara, *Science* **1997**, *277*, 1074–1077.
- [3] R. M. Dickson, A. B. Cubitt, R. Y. Tsien, W. E. Moerner, *Nature* **1997**, *388*, 355–358.
- [4] M. Nirmal, B. O. Dabbousi, M. G. Bawendi, J. J. Macklin, J. K. Trautman, T. D. Harris, L. E. Brus, *Nature* **1996**, *383*, 802–804.
- [5] M. Kuno, D. P. Fromm, H. F. Hamann, A. Gallagher, D. J. Nesbitt, *J. Chem. Phys.* **2001**, *115*, 1028–1040.
- [6] M. Lippitz, F. Kulzer, M. Orrit, *ChemPhysChem* **2005**, *6*, 770–789.
- [7] J. Cui, A. P. Beyler, T. S. Bischof, M. W. B. Wilson, M. G. Bawendi, *Chem. Soc. Rev.* **2014**, *43*, 1287–1310.
- [8] A. Swarnkar, R. Chulliyil, V. K. Ravi, M. Irfanullah, A. Chowdhury, A. Nag, *Angew. Chem. Int. Ed.* **2015**, *54*, 15424–15428; *Angew. Chem.* **2015**, *127*, 15644–15648.
- [9] V. V. Protasenko, K. L. Hull, M. Kuno, *Adv. Mater.* **2005**, *17*, 2942–2949.

- [10] J. J. Glennon, R. Tang, W. E. Buhro, R. A. Loomis, *Nano Lett.* **2007**, *7*, 3290–3295.
- [11] Y. Tian, A. Merdasa, M. Peter, M. Abdellah, K. Zheng, C. S. Ponseca, T. Pullerits, A. Yartsev, V. Sundström, I. G. Scheblykin, *Nano Lett.* **2015**, *15*, 1603–1608.
- [12] H. Yuan, E. Debroye, G. Caliandro, K. P. F. Janssen, J. van Loon, C. E. A. Kirschhock, J. A. Martens, J. Hofkens, M. B. J. Roelfaers, *ACS Omega* **2016**, *1*, 148–159.
- [13] S. Wang, C. Querner, T. Emmons, M. Drndic, C. H. Crouch, *J. Phys. Chem. B* **2006**, *110*, 23221–23227.
- [14] P. Frantsuzov, M. Kuno, B. Jankó, R. A. Marcus, *Nat. Phys.* **2008**, *4*, 519–522.
- [15] Y. E. Panfil, M. Oded, U. Banin, *Angew. Chem. Int. Ed.* **2018**, *57*, 4274–4295; *Angew. Chem.* **2018**, *130*, 4354–4376.
- [16] J. Si, S. Volkán-Kacsó, A. Eltom, Y. Morozov, M. P. McDonald, M. Kuno, B. Jankó, *Nano Lett.* **2015**, *15*, 4317–4321.
- [17] W. Xu, W. Liu, J. F. Schmidt, W. Zhao, X. Lu, T. Raab, C. Diederichs, W. Gao, D. V. Seletskiy, Q. Xiong, *Nature* **2017**, *541*, 62–67.
- [18] D. Shi, V. Adinolfi, R. Comin, M. Yuan, E. Alarousu, A. Buin, Y. Chen, S. Hoogland, A. Rothenberger, K. Katsiev, Y. Losovyj, X. Zhang, P. A. Dowben, O. F. Mohammed, E. H. Sargent, O. M. Bakr, *Science* **2015**, *347*, 519–522.
- [19] W. Tian, C. Zhao, J. Leng, R. Cui, S. Jin, *J. Am. Chem. Soc.* **2015**, *137*, 12458–12461.
- [20] A. Merdasa, Y. Tian, R. Camacho, A. Dobrovolsky, E. Debroye, E. L. Unger, J. Hofkens, V. Sundström, I. G. Scheblykin, *ACS Nano* **2017**, *11*, 5391–5404.
- [21] A. Halder, R. Chulliyil, A. S. Subbiah, T. Khan, S. Chatteraj, A. Chowdhury, S. K. Sarkar, *J. Phys. Chem. Lett.* **2015**, *6*, 3483–3489.
- [22] L. Dou, A. B. Wong, Y. Yu, M. Lai, N. Kornienko, S. W. Eaton, A. Fu, C. G. Bischak, J. Ma, T. Ding, N. S. Ginsberg, L. W. Wang, A. P. Alivisatos, P. Yang, *Science* **2015**, *349*, 1518–1521.
- [23] W. Tian, R. Cui, J. Leng, J. Liu, Y. Li, C. Zhao, J. Zhang, W. Deng, T. Lian, S. Jin, *Angew. Chem. Int. Ed.* **2016**, *55*, 13067–13071; *Angew. Chem.* **2016**, *128*, 13261–13265.
- [24] B. Wu, H. T. Nguyen, Z. Ku, G. Han, D. Giovanni, N. Mathews, H. J. Fan, T. C. Sum, *Adv. Energy Mater.* **2016**, *6*, 1600551.
- [25] T. S. Sherkar, C. Momblona, L. Gil-Escrig, J. Ávila, M. Sessolo, H. J. Bolink, L. J. A. Koster, *ACS Energy Lett.* **2017**, *2*, 1214–1222.
- [26] A. Halder, N. Pathoor, A. Chowdhury, S. K. Sarkar, *J. Phys. Chem. C* **2018**, *122*, 15133–15139.

Manuscript received: April 26, 2018

Revised manuscript received: May 30, 2018

Accepted manuscript online: July 11, 2018

Version of record online: August 7, 2018